Applied Energy 264 (2020) 114724

Contents lists available at ScienceDirect

Applied Energy

journal homepage: www.elsevier.com/locate/apenergy

Quantifying seasonal and diurnal contributions of urban landscapes to heat energy dynamics

Zhaowu Yu[a,b,c,*], Tingting Chen[a,d,1], Gaoyuan Yang[b], Ranhao Sun[a,*], Wei Xie[a], Henrik Vejre[b]

[a] State Key Laboratory of Urban and Regional Ecology, Research Center for Eco-Environmental Sciences, Chinese Academy of Sciences, Beijing 100085, China
[b] Department of Geosciences and Natural Resource Management, Faculty of Science, University of Copenhagen, Rolighedsvej 23, 1958 Copenhagen, Denmark
[c] Shanghai Key Lab for Urban Ecological Processes and Eco-Restoration, Shanghai, China
[d] School of Life Sciences, University of Science and Technology of China, Hefei 230022, China

HIGHLIGHTS

- Numerical contributions of typical landscapes to sensible heat flux are quantified.
- Changes in sensible heat flux during the diurnal and season are quantified.
- Controversial results based on remote sensing data are partly resolved.
- The difference in sensible heat flux of typical landscapes is the greatest at 2 pm.

ARTICLE INFO

Keywords:
Urban landscape
Sensible heat flux
Contribution rate
Diurnal and seasonal variation
Climate adaption
Cooling energy saving

ABSTRACT

Cooling energy consumption in urban areas is affected significantly by the dynamics of urban heat flux. However, we still lack a clear understanding of the quantitative contribution rate and underlying mechanism of typical urban landscapes to urban heat dynamics, especially in seasonal and diurnal patterns. Here we used a thermal infrared camera and portable meteorological instruments to examine the sensible heat flux (SHF) changes of five typical urban landscapes in Beijing based on surface temperature and concurrent microclimate conditions. Diurnal and seasonal variations of SHF were quantified by comparing changes in forenoon and afternoon in different seasons. Results showed that (1) walls and roads act as heat-source, while forests and water act as heat-sink in all seasons; however, grassland served as heat-sink in summer and spring-autumn, but it becomes a heat-source in winter. (2) The seasonal variation of sensible heat flux of the wall is the greatest, followed by water, while that of trees is the smallest. Besides, the highest sensible heat flux and the maximum variation among typical urban landscapes occur between noon and 2:00 pm. (3) The numerical contribution rate of typical landscapes to sensible heat flux varies with daytime (forenoon and afternoon) and seasonal changes, and these ratios can be used as parameters to adjust the numerical models to obtain more reliable results in surface-energy-flux-related studies. The results of this study can provide a reference for explaining controversial findings based on remote-sensing data, and provide insights into revealing the sensible heat flux mechanism of typical urban landscapes and cooling energy conservation in cities.

1. Introduction

Heat fluxes of urban landscapes vary in different times and seasons and these energy dynamics affect the thermal comfort of urban residents. Previous studies usually focus on the urban heat island (UHI) effect which is defined as the phenomenon of urban temperatures being higher than those in the rural surroundings [1,2]. In general, the UHI effect is mainly caused by changes in the urban landscape [3] and spatial structure (spatial dimensions of buildings and street canyons) [4], surface physical properties [2], air pollution [5], and anthropogenic heat emission [6]. It is apparent that urbanization is the main driving force of these changes. Urbanization has significantly transformed natural and semi-natural surfaces into artificial impervious surfaces and urban infrastructures such as concrete, asphalt, masonry,

* Corresponding authors at: Assistant professor in University of Copenhagen, study about Urban Ecology, Landscape Ecology and Climate Adaption Planning (Z. Yu); Professor in Landscape Ecology and Ecosystem Services (R. Sun).
E-mail addresses: zhyu@ign.ku.dk (Z. Yu), rhsun@rcees.ac.cn (R. Sun).
[1] The co-first author.

https://doi.org/10.1016/j.apenergy.2020.114724
Received 2 January 2020; Received in revised form 18 February 2020; Accepted 21 February 2020
Available online 29 February 2020

and metal alter the surface aerodynamic properties of the urban landscape as well as the balance of heat and energy within urban areas [2,7–9]. For instance, impervious surfaces usually absorb more solar radiation and have a greater heat capacity and thermal conductivity as compared to natural surfaces [1,10,11]. The physical properties (e.g., albedo, emissivity, thermal capacity, thermal conductivity, and thermal inertia) and humidity characteristics of the different landscapes vary widely and significantly affect the surface energy balance, which, in turn, affects the urban thermal pattern and heterogeneity [2,12,13]. In a review study, Santamouris (2014) found that the UHI effect cause an increase in the ambient temperature and modifies the energy budget of buildings; furthermore, on average, the cooling load of typical urban buildings are 13% higher than that of similar buildings in rural areas [7]. Hence, it is clear that the UHI effect can significantly increase the cooling energy (and water) consumption [14,15] and reduce the sensible heat released—that is, weaken the atmospheric heating process. Hence, slowing down the UHI effect is a scientific consensus [1,8,16]. Therefore, quantifying the sensible heat flux (SHF) release of different typical urban landscapes has important and practical significance on cooling energy saving (i.e., reducing the demand for cooling energy) [17,18] and thermal environment improvement [10,19].

Recent studies have found that buildings (walls) and roads contribute significantly to SHF [2,14]; in contrast, green vegetation and water can cool a built environment via shading and the evapotranspiration effect, thus contribute to cooling energy saving [17,20,21]. For instance, Kuang et al. (2015) found that the land surface temperature (LST) of an impervious surface is approximately 6–12 °C higher than that of urban green spaces, and this difference can be attributed to various fractions of sensible heat or latent heat flux [22]. Hence, the natural surface of a green (vegetation) space can be regarded as a natural air-conditioner and can reduce the energy consumption of buildings, especially on hot summer days [17,23,24]. Besides, Chudnovsky et al. (2004) analyzed the surface temperature changes of different objects in the city of Tel Aviv [25], and Hoyano et al. (1999) analyzed the SHF from the exterior surface of buildings using time-sequential thermography in Osaka [26]. In these studies, the quantitative contribution rate of typical urban landscapes to SHF is still unclear, especially with respect to seasonal and diurnal patterns [3,20]. This limits the understanding of the cooling effect of urban landscape types and, in turn, affects the understanding of cooling energy consumption [18,23]. For instance, whether the cooling effect (SHF) of grassland is negative or positive, and what is the difference in the effect of seasonal and diurnal patterns on the cooling effect (SHF) of grassland are controversial issues in this field?

While considering various perspectives, Miao et al. (2014) [27] analyzed the urban heat balance using vorticity-related data and the mesoscale meteorological weather research and forecasting model as well as the urban canopy model. It is apparent that the vorticity correlation method records long- and short-wave radiation in different directions, which can be used to accurately calculate the value of each component of the thermal equilibrium [28]. However, the types of urban surface landscapes are complex, and vorticity-related data on mixed surface types cannot reflect the heat radiation characteristics of a single surface; thus, it is difficult to distinguish different surface heat radiation fluxes. Therefore, it is necessary to use finer data and appropriate methods to explore the SHF pattern and mechanism to determine the environmental cooling and energy-saving potential. To date, with the exception of the above (modeling) method, UHI (SHF) studies have often been conducted using three methods, including the use of air-temperature measurements from weather stations, field observations of surface radiant temperatures using portable infrared thermometers or thermal infrared imagers, and land surface temperatures (LSTs) retrieved from satellite remote sensing (RS) images which have been widely used in recent decades [19,29,30]. In general, historical data can be retrieved from fixed meteorological stations, but owing to the limited number of meteorological stations, it is difficult to obtain detailed temperature information for a given city [2,21]. It is also difficult to analyze the generation mechanism and energy change of UHIs [28]. RS-based products can be used to quantify the spatial characteristics of SHF on different urban surfaces, but they are limited by low temporal resolutions and short data records in addition to difficulties in validating the retrieved results [29,31,32]. Moreover, RS data cannot capture the complex three-dimensional structure of a city, and its geometric features are often generalized into two-dimensional surfaces; thus, the urban canopy, which has a significant impact on the urban thermal environment, is insufficiently characterized [28]. More importantly, the inherent limitations of RS-based data (e.g., RS can only capture SHF) cause challenges in resolving some critical controversies such as those previously mentioned. These issues have been discovered in previous RS-based studies; however, these controversies cannot be resolved only using RS data [3,19,33].

Field measurements usually involve the use of portable infrared thermometers or thermal infrared images, which can provide more information (timely and accurate) for measuring the status of the local thermal environment and energy changes [17,28]. Therefore, to address the problems of the above-mentioned methods in calculating urban surface heat fluxes, especially SHF, the objective of this study is to use a thermal infrared camera and portable meteorological instruments to simultaneously record SHF in three directions. Although some previous studies also used thermal infrared cameras and other methods to capture the SHF characteristics in small-scale urban landscapes [17,22,28], there exist rare studies in which the seasonal and diurnal patterns of SHF in typical urban landscapes have been investigated. Furthermore, studies have rarely been attempted to quantify the contribution rate of SHF in different seasons and diurnals in typical urban landscapes. This has limited the understanding of the SHF mechanisms and resulted in the controversies remaining unresolved (RS-based data and on-site measurement data) [21].

Therefore, to address these insufficiencies, Beijing was selected as the case study area because of its typical rapid urbanization and serious thermal environmental problems (i.e., UHI and heatwave) [6,34]. The basic logic of this study is that we can take better measures to alleviate the UHI effect only by clearly understanding the SHF of different landscapes, and we can then reduce cooling energy consumption. Hence, the objectives of this study are to (1) quantify the seasonal and diurnal patterns in terms of the contributions of typical urban landscapes to SHF, (2) determine the contribution rate of SHF over time in different urban landscapes, and (3) further investigate the controversies caused by RS-based data by comparing the differences in SHF in different urban landscapes in different seasons. This study would enhance the understanding of SHF mechanisms and provide an explanation for previous controversial findings in addition to providing parameters for use in surface energy flux related studies.

2. Materials and methods

2.1. Study area site

In this study, based on the detailed survey of the functional zones within the Beijing Fifth Ring Road, three sites (Fig. 1) were selected to represent the typical functional area of the city: the Sinosteel International Plaza, Research Center for Eco-Environmental Sciences at the Chinese Academy of Sciences (RCEES), and Olympic Forest Park, which represent the commercial functional, educational functional, and ecological functional areas, respectively. The urban landscape types of the experimental sites included road surfaces, grassland (unirrigated), trees, buildings, and water bodies. The road surface comprised road surface brick. In addition, the walls of the buildings selected for this study were south facing.

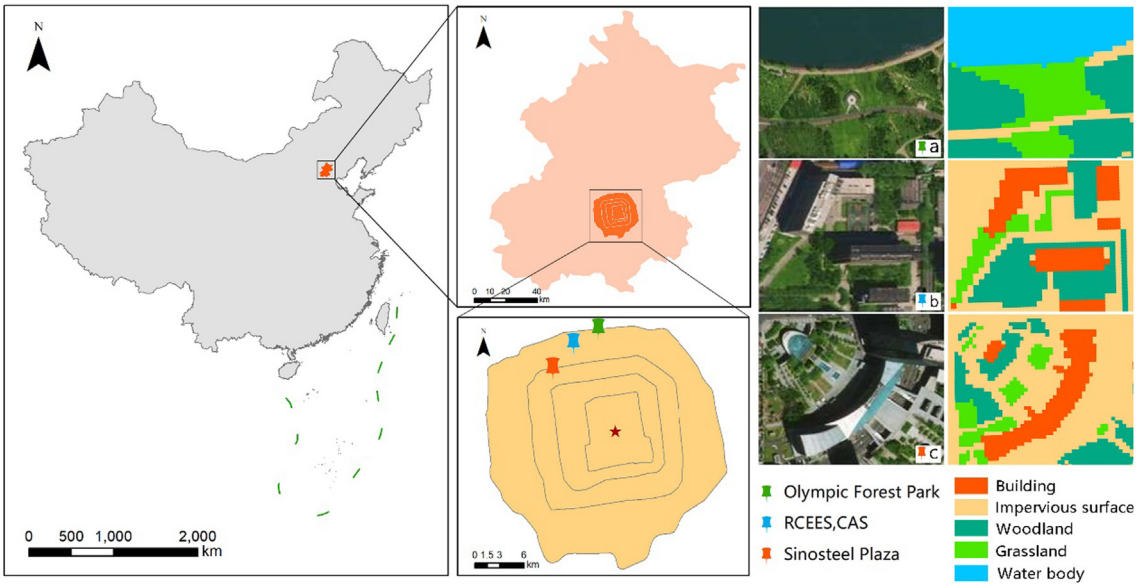

Fig. 1. Study sites in Beijing (a: Olympic Forest Park; b: Research Center for Eco-Environmental Sciences, Chinese Academy of Sciences (RCEES, CAS); and c: Sinosteel International Plaza).

2.2. Surface temperature measurements

A thermal infrared camera (Testo-890) was used to capture thermographs (Fig. 2 shows the example of the images captured using the Testo-890 thermal infrared camera at different study sites). Table 1 provides information regarding the thermal camera, the WatchDog, and Kestrel's technical specifications. The thermal infrared camera used in this study can simultaneously obtain the surface temperature at a large number of points. Therefore, surface temperature measurements can be taken over the entire study site, rather than at only one point. Three field tests were conducted at different study sites to evaluate the contributions of the different urban landscapes. The thermal infrared camera was installed at the highest point in the region. The camera remained at a constant position at each monitoring location. The measurements were conducted at 1-h intervals from 8:00 am to 4:00 pm on days that were sunny and cloudless with light winds (wind speed < 2 m/s) in March, April, July, August, and September of 2016. The selected days and detailed meteorological information are listed in *Table S1, Supplementary Materials.*

2.3. Calibration of measured surface temperatures

The emissivity value in this study was between 0.85 and 0.95. According to a previous study, the difference between the measured and actual temperature is insignificant if the emissivity setting error is < 0.1 [35]. In addition, the difference is only 0.6 °C when the distance is 100 m [35], and the greatest distance in this study is less than 100 m. Thus, there is no calibration of the surface temperature and 0.90 was selected as the emissivity in this study.

2.4. Calculation model of sensible heat flux

The WatchDog and Kestrel were used to record the air temperature and humidity at a height of 1.5 m. The SHF is the heat transferred from the surface to the air, which is related to the difference between the surface temperature (ST) and air temperature (AT). As the temperature difference increases, the transfer potential of the sensible heat to the atmosphere increases. The SHF is released into the atmosphere via convection, and the air velocity has great influence on this process. In addition, as the wind speed increases, the surface air turbulence increases, and the sensible heat transfer increases. Therefore, the sensible heat can be estimated based on the surface temperature (ST), air temperature (AT), and wind speed. It should be mentioned that owing to instrument limitations, there is no simultaneous monitoring of air temperatures at different height of the (building) wall, and air temperatures were calculated at different heights based on the equations proposed by Sham, Memon [36].

The sensible heat flux (W/m^2) release was calculated using Eq. (1) [26,28,37]. In this equation, T_s is the surface temperature (°C), T_a is the air temperature (°C), and h_c (W/(m^2 °C) is the air turbulence coefficient, which was calculated using Eq. (2).

$$H = h_c (T_s - T_a) \quad (1)$$

$$h_c = \begin{cases} 5.6 \times 4.0 & v < 5 \\ 7.2 \times v^{0.78} & v \geq 5 \end{cases} \quad (2)$$

In Eq. (2), the wind speed v (m/s) is measured at 9 m above the Earth's surface; however, in this study, the wind speed observations were collected at a height of 1.5 m. To obtain the required wind speed at the appropriate height, a wind speed conversion was conducted using the wind profile index rate, as shown in Eq. (3) [38].

$$u_z = u_1 \left(\frac{Z}{Z_1} \right)^{\alpha} \quad (3)$$

In Eq. (3), u_z is the wind speed (m/s) at the height of z, u_1 is the wind speed at the known height, and Z (m) and Z_1 (m) are the corresponding heights, respectively. α is a constant value and is correlated with surface roughness. It can be represent as the $\alpha = 0.12\ Z_0 + 0.18$ [28,38]. The surface roughness in an urban area with a height of 2 m is 0.42, and hence $\alpha = 0.23$ in this study.

The ratio of SHF is calculated from the area between line and X-axis.

2.5. Statistics analysis

In this study, with the employment of IBM SPSS 21 software, we also used a variance analysis to determine the contribution of different urban landscapes to the thermal environment. Besides, seasons are divided into three categories, including summer, winter, and spring-autumn, and the variation of the contributions of different landscape types in the three seasons was analyzed. The Levene test ($p \leq 0.05$) indicated that the population variance was not equal; thus, Welch's *T*-test was used in the variance analysis process. Welch's *t*-test is a two-sample

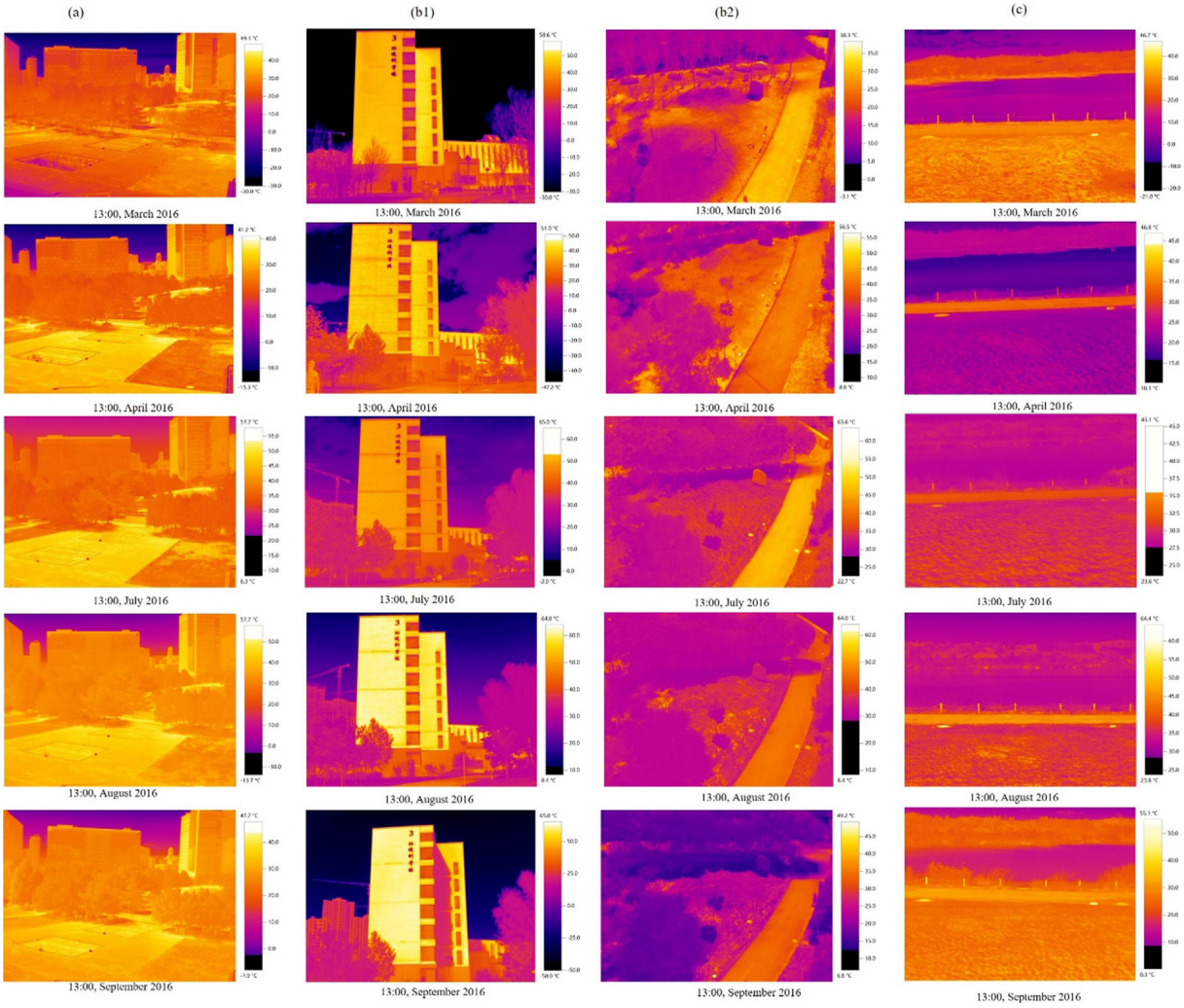

Fig. 2. Images obtained using the Testo-890 thermal imaging camera in different months (March, April, July, August, and September) at 1:00 pm (local time). a: Sinosteel International Plaza; b: Research Center for Eco-Environmental Sciences at the Chinese Academy of Sciences; c: Olympic Forest Park.

Table 1
Thermal camera (Testo-890), WatchDog, and Kestrel technical specifications.

Testo-890	IR resolution	640 × 480 pixels
	Field of view (FOV)	42° × 32°/0.1 m
	Spatial resolution (IFOV)	1.13 mrad
	Thermal sensitivity	< 40 mK at +30 °C
	Image frequency	33 Hz
	Temperature range	−30 °C to +100 °C
	Accuracy	± 2 °C or ± 2% of reading
WatchDog B100	Temperature range	−40 °C to +85 °C
	Accuracy	± 1 °C (−30 °C to +70 °C)
Kestrel 3000	Wind speed range	0.6–60 m/s
	Resolution	0.1 m/s
	Accuracy	Better than ± 3% of reading

location test that is used to test the hypothesis that two populations have equal means, and it is more reliable when the two samples have unequal variances and/or unequal sample sizes. In addition, the Dunnett's T3 test (Dunnett's T3 is a pairwise comparison test based on the studentized maximum modulus. This test is appropriate when the variances are unequal.), which does not assume equal variance between groups, was used as the post hoc test method. Furthermore, significant differences were obtained between the different landscape types at the 0.05 level.

3. Results

3.1. Surface temperature variations of different urban landscapes

The surface temperature (ST) and SHF were compared at the different study sites. The results showed that the ST (and SHF) of different typical urban landscape types have no significant effect in different study sites, which means that the location (functional zone) of different urban landscapes does not generally affect the ST and SHF. Fig. 3 shows the surface temperatures of five typical landscape types and indicates that the ST of the walls and roads is the highest during all seasons, especially from 12:00 noon to 2:00 pm. The reasons for this result are that solar radiation is the highest during this interval and also the thermal properties of the wall and road. In addition, Fig. 3 shows that water has the lowest ST during all seasons and at almost all times (except in the morning), which can be attributed to the specific heat capacity of water. In general, it can be observed that roads and walls in urban landscapes are the heat sources of the cities, and the green vegetation and water bodies are the heat sinks.

3.2. Seasonal and diurnal variations in SHF for different urban landscapes

Fig. 4 shows the SHF changes during the daytime for different typical urban landscapes. The results show that the diurnal variation of the SHF from the road is the same across different seasons; however, the

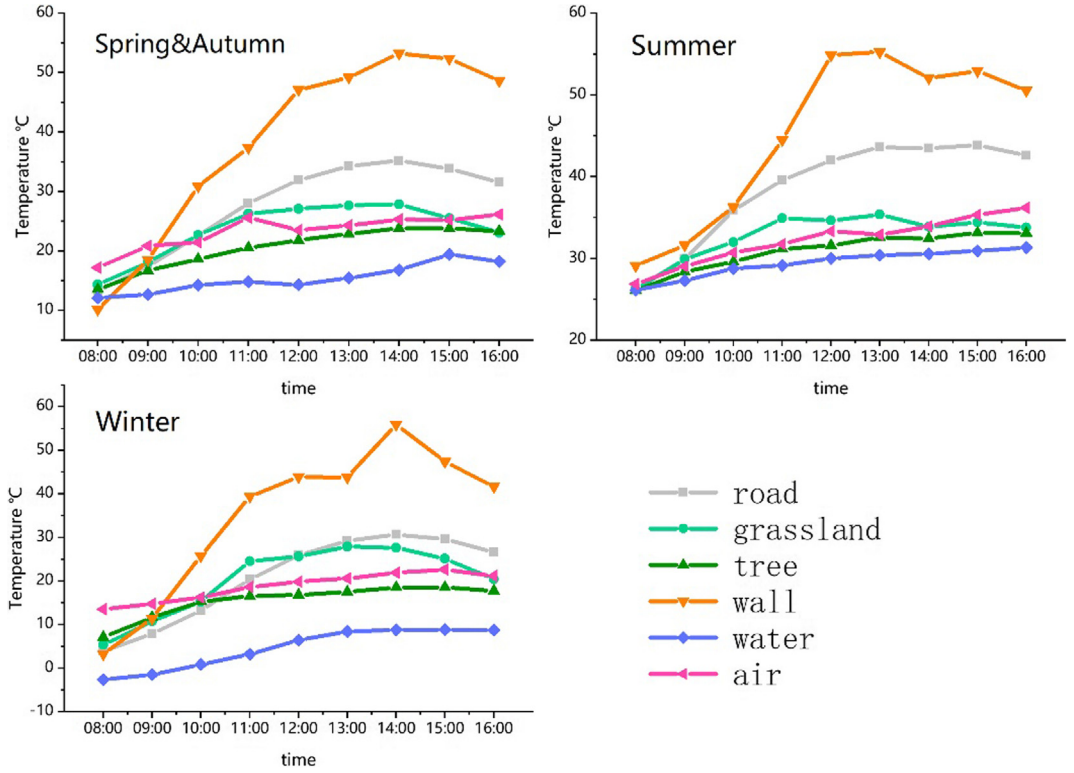

Fig. 3. Surface temperature and corresponding air temperature for different typical landscapes in different seasons.

SHF varies greatly in the morning and is low in the afternoon. In summer mornings, roads release the highest amount of SHF as compared to that in winter, and we believe these results are directly related to the amount of solar radiation received by the road surface (summer being the season with the most solar radiation). The SHF ratio of roads in different seasons (spring-autumn, summer, and winter) is 1:1.5:1.

Fig. 4 also shows that, in summer, the diurnal variation of the SHF of the wall first increases and then decreases (1:00 pm). This pattern is obtained owing to changes in solar radiation. The diurnal variation trends of the SHF in spring–autumn and winter are nearly identical and

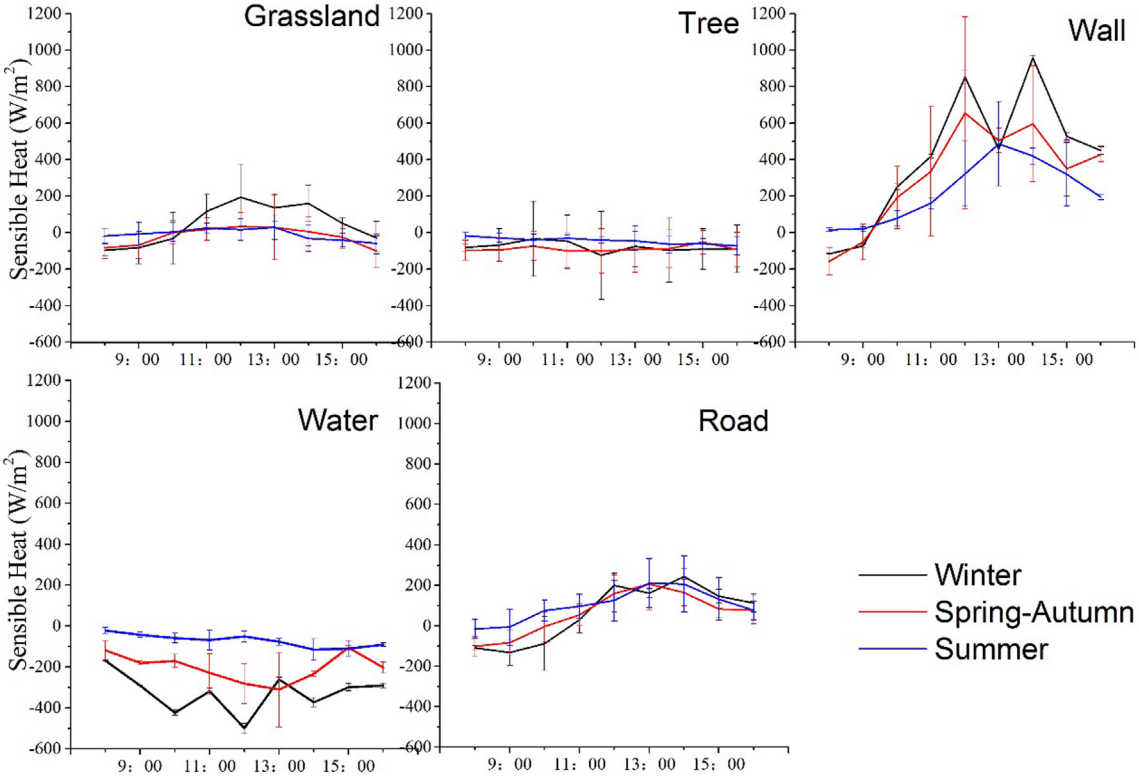

Fig. 4. Changes in SHFs of various urban landscapes during different seasons.

forms an “M” shape. There are short-lived clouds in the observations of spring-autumn, and winter, and we opine that this is the main reason for this pattern. Generally, we opine that the SHF results of spring–-autumn and winter should be the same as those of the summer season. In addition to the changes observed from 9:00 to 10:00 am and at 1:00 pm, the SHF of the walls varies greatly in each season. The wall surface considered in the experiment comprised concrete and masonry with dark-gray paint and the wall is facing south. In contrast to other urban landscapes, the amount of sensible heat released by the wall (south) is the greatest in winter and the lowest in summer. The SHF ratio of walls in different seasons (spring-autumn, summer, and winter) is 1:0.7:1.3.

Fig. 4 shows that the daytime ST of the green vegetation is lower than that of other urban landscapes, and the SHF is generally negative, which indicates that the green vegetation has a cooling effect. This is mainly because of the loss of latent heat energy caused by plant transpiration. In general, the SHF of the grassland remains steady at close to zero in different seasons, except in the case of winter afternoons. The reason for the high SHF of grassland in winter is the growth of vegetation. As the observed grassland fades in winter, bare soil can be observed on the grassland, which changes the thermal characteristics of the grassland and results in a change in the SHF. The SHF ratio of grassland in different seasons (spring-autumn, summer, and winter) is $-1:-0.4:4.7$. The diurnal variation of the SHF of trees is similar to that of grassland but exhibits a lower SHF value, which means that trees have better cooling effects. The SHF ratio of trees in different seasons (spring-autumn, summer, and winter) is $-1:-0.5:-0.9$.

Fig. 4 shows that the diurnal variation of the SHF of water is generally stable, but the SHF fluctuates in spring–autumn and winter. In addition, the results show that the SHF of water in different seasons is quite varied; the SHF is highest in summer and lowest in winter. These results indicate that water always acts as a “cold island” in the city and plays an important role in cooling the surrounding environment. Furthermore, as compared to green vegetation, it can be observed that water has a better cooling effect in terms of SHF reduction. The SHF ratio of water in different seasons (spring-autumn, summer, and winter) is $-1:-0.3:-1.6$.

In this section, we can conclude that the impact of typical urban landscapes on the thermal environment changes over time. Therefore, the subsequent analysis of differences between different urban landscapes should include different times of day and seasons (Section 3.3).

3.3. SHF variations among different urban landscapes

To quantify the impact of the different urban landscapes to the thermal environment, the SHF and its average value at different times (diurnal and seasonal) were calculated (Fig. 5). The results show that the highest SHF is obtained from the wall (south); the second-highest SHF from the road, and the lowest SHF from the water. These results suggest that owing to the complexity of the urban environment, there is a large difference in sensible heat at the microscale. Walls and roads are heat sources, while water bodies and green vegetation are generally heat sinks. In particular, the results show that water bodies are most effective in reducing the SHF. It can be observed that the impact of urban landscapes on the thermal environment changes over time. For instance, during the experiment, the highest sensible heat difference between urban landscapes occurred in the afternoon (12:00 noon–2:00 pm, local time), which is the time at which the sensible heat reaches its daily maximum. Therefore, it is necessary to analyze the results obtained for the three-time periods of day and morning from 8:00 am to 12:00 noon and from 12:00 noon to 4:00 pm. We calculated the ratio of each landscape's contribution to the urban thermal environment in the corresponding period. The results are presented in Fig. 5. Furthermore, walls and roads represent artificial landscapes, while grassland, trees, and water represent natural landscapes in the next analysis.

In spring-autumn, according to the results of the variance analysis, no significant difference was observed (at the 0.05 level) between the wall and the road during the entire daytime period, while significant differences were observed between the tree and water. In addition, there were significant differences between different urban natural landscapes. The thermal environment contribution rate ratio of roads, grassland, trees, walls, and water is $5.6:-1:-7:27:-16.5$. In the morning, in particular, there is a big difference between water and the other urban landscapes, and the SHF ratio of different urban landscapes of roads, grassland, trees, walls, and water is $-1:-17.9:-88.1:172.6:-185$. In addition, the SHF of different urban landscapes are quite different in the afternoon and is characterized by the smallest and largest SHF of water and wall surface, respectively. Furthermore, the SHF ratio of roads, grassland, trees, walls, and water is $22.1:-1:-12.7:76.6:-34.2$.

The variance analysis for summer shows that there is no significant difference between the SHF of the wall and the road during the entire daytime period. However, there are remarkable differences in the SHF of different natural landscapes such as grass and water, which vary widely. The contribution rate of roads, grassland, trees, walls, and water to the thermal environment is $19:-1:-7.7:41.6:-12.5$. In the morning, in particular, there is no significant difference between the SHF of the road and the wall, but a significant difference has been found between that of the road, trees, and water. Furthermore, the variance analysis presented considerable differences between the SHF of the walls and natural landscapes and between the water and other natural landscapes. The contribution rate of roads, grassland, trees, walls, and water to the thermal environment is $10.5:1:-6.1:20.3:-9.8$. In the afternoon, the SHF of the roads and walls differs greatly, and all the SHF values are significantly different from those of the natural landscapes. In addition, the SHF of grassland and other natural landscapes is also very different in the afternoon. The contribution rate of the roads, grassland, trees, walls, and water to the thermal environment is $9.7:-1:-3.4:22.1:-5.5$.

The variance analysis for winter shows that there is no significant difference between the SHF of walls and roads, but there is a significant difference between that of trees and water. The contribution rate of the roads, grassland, trees, walls, and water to the thermal environment is $1.2:1:-1.3:7.4:-5.6$. In the morning, in particular, there is a significant difference between the SHF of the roads and walls. Moreover, there is a large difference between the SHF of the artificial landscape and water, as well as a big difference between the SHF of water and other urban natural landscapes. The contribution rate of the roads, grassland, trees, walls, and water to the thermal environment is $-2.9:1:-5.1:19.3:-27.3$. We consider anthropogenic heat emissions to be the reason for the positive contribution of the walls to the thermal environment during winter mornings at the study site. In the afternoon, there is a significant difference between all the urban landscapes, and the contribution rate of roads, grassland, trees, walls, and water to the thermal environment is $1.9:1.2:-1:7:-3.6$. We consider that the reasons for this pattern are solar radiation and thermal properties as well as anthropogenic heat emissions.

4. Discussion

4.1. Mechanism of typical urban landscapes to heat dynamics

The mechanism of urban heat dynamic has always been an important aspect of urban climate and thermal environment research [2,8]. In the early 1990s, many related studies were based on surface energy balance (SEB) models [35]; and the heat released by urban landscapes (i.e., green vegetation, building and road materials) are mainly referred to as the residual of the SEB equation, or the heat obtained through simulation models such as TAS and ENVI-met [7,17,39]. In recent years, studies are paying more and more attention to the heat dynamic processes and mechanisms of typical urban landscapes

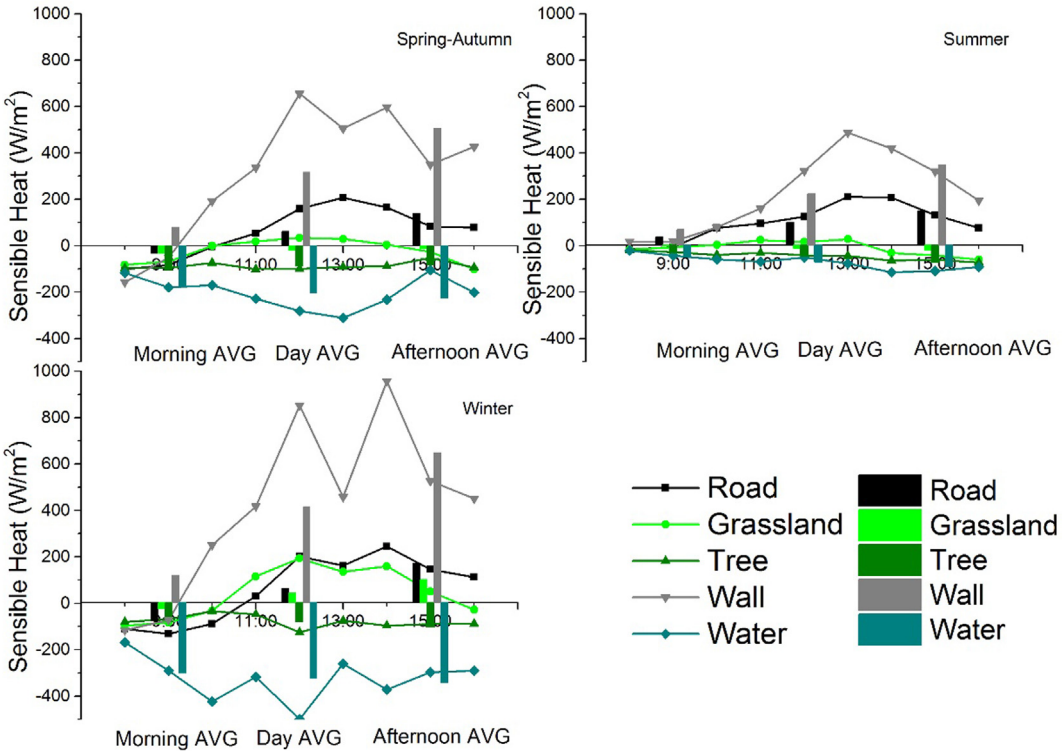

Fig. 5. Sensible heat fluxes of different urban landscape types. In this study, the daytime is divided into three periods: morning, noon(day), and afternoon. AVG means average SHF.

[18,27,34]. Within that, LST and surface temperature plays a key role in bridging different urban landscape and heat energy dynamic (budge) [22,32,35,40].

In general, previous studies have revealed that since cities are mainly composed of impervious surfaces of concrete, asphalt, bricks or aggregates, they absorb and store radiation during the day and slowly release heat at night [1,2]. Specifically, impervious surfaces and building fabrics have higher thermal conductivity and capacity, so they can absorb more incident solar energy and release the absorbed energy as SHF into the air especially at night, resulting in higher ambient temperatures [22,35]. For instance, light-colored surface materials (i.e., building and road) usually have higher albedo and absorb less heat, while dark-colored materials usually absorb more heat than light-colored materials, resulting in higher SHF emission [2,10,22]. In contrast, vegetated surfaces (i.e., tree and grassland) have a high evapotranspiration (and shading) potential and can selective absorption and reflection of incident radiation and the regulation of latent and sensible heat exchange, resulting in lower surface temperature [18,20]. In addition, compared to impervious surfaces, vegetation and water bodies have low thermal conductivity and high heat capacity, so they can slowly release heat energy into the air [21]. Hence, it is obvious that the difference in the thermal properties of the different surfaces is the basic mechanism leading to the urban heat dynamics; and these differences were also verified in this study.

More specifically, many previous studies have revealed the heat dynamic of the different urban landscapes [2,17,20]. For instance, in Beijing case, Kuang, Liu [22] found that the components of the net between urban impervious surface, green space, and cropland were significantly different. By observing surface radiation and heat flux, they also revealed that the difference was caused by different fractions of the sensible or latent heat flux in the net radiation. In Indianapolis, Weng, Liu [40] also found that the net radiation of cropland is greater than that of green space, and the green space is greater than the urban impervious surface, which is consistent with our research. What is more, in this study, we quantified the ratios of SHF in typical urban landscapes in a diurnal and seasonal pattern. This further deepens our understanding of the mechanism of heat dynamics in the typical urban landscapes, and it can be a valuable reference for explaining controversial findings based on RS data and improving the accuracy of the urban surface energy flux numerical model.

4.2. Research implications: Theoretical and practical

4.2.1. Comparison of results obtained based on RS data and on-site measurement data

As is known to us, RS-based LST – which usually reflects the sensible heat release of the landscape—has been widely used to study the effects of different urban landscapes on the UHI pattern in recent decades [29,41,42]. It is apparent that the RS-based LST data significantly deepens the understanding of the landscape patterns and processes and their effects on large spatial and temporal scales [9,11,43]. However, the limitations (as mentioned above) of RS-based data make it challenging to find underlying mechanisms for these changes and effects (which, in turn, limit the understanding of cooling energy saving) as well as to explain controversial results. In this study, we used on-site measurement and observation data to calculate the SHF for different urban landscapes, compare the results of the RS-based data, identify the mechanisms behind it, and answer the corresponding controversial scientific questions.

In line with the previous RS-based results [13,22,34], this study further confirmed that the impervious surfaces, such as roads and walls, have a higher surface temperature (ST) and SHF during the daytime, while trees (grassland) and water have a lower ST and SHF. These results indicate that the urban landscapes of roads and walls are heat sources, while water and green vegetation are heat sinks; by controlling the heat release from walls and roads (anthropogenic heat emissions), an increase in the proportion of water and green vegetation areas can result in an improvement in urban thermal environments [1,42,44,45]. The study clearly found that water has the lowest ST and SHF during the daytime during different seasons as compared to green vegetation,

which in accordance with the results of some previous RS data-based studies [31,46,47]. The main reason for this obtained result is that water has a higher specific heat capacity than green vegetation. However, some studies have also found that seasonal patterns affect the LST between green vegetation and water. For instance, in a case (1987–2010) from Shanghai, China, it was found that the cooling effect of the green vegetation in May is stronger than that of the water body, while the water cooling effect in November is stronger than that of the green vegetation [33]. Conversely, Gunawardena et al. [48] pointed out that the transpiration-based cooling effect of green and blue space is primarily relevant for urban canopy-layer conditions and that the tree-covered green space offers the greatest heat-stress relief. More importantly, based on the literature analysis, we found that the studies based on field measurement data (air temperature) generally states that the cooling effect of trees is better than that of water [21,49,50]. These results can be explained by the cooling mechanisms of trees, which include the regulation of SHF and latent heat fluxes, as well as the shading effect of trees [8,51]. Therefore, when we compare the results of our research with others, it is necessary to consider the data source used and the difference between air temperature, surface temperature, land surface temperature, and the sensible and latent heats [21]. Otherwise, the results cannot be compared, and their comparison could cause a novice reader to obtain a wrong understanding.

In addition, this study found that as compared to the green vegetation of trees, grassland showed a warming effect (SHF is positive) in the winter, and the SHF of grassland is close to zero in other seasons. The cause of this phenomenon is the growth of grassland and trees. Beijing is located in a temperate continental monsoon climate, wherein the grassland is withered in winter, and some grassland even turns into bare land owing to human trampling, which changes the thermal properties of the grassland and eventually changes its SHF. Furthermore, previous RS based [3], field measurement based [52], and numerical model based [18] studies have found that grassland is not always a heat sink and even presents as a heat source. Yu et al. (2018) [32] even found that the cooling effect of grassland is highly correlated with the climate conditions: as compared with the cities in temperate climate zones, the cooling effect of grassland in Mediterranean cities is highly dependent on precipitation. This can be explained by the cooling mechanism (transpiration) of grassland: the transpiration in a dry area relies heavily on the water supply [18,19]. In short, this study confirmed the accuracy of the conclusions based on RS data that grassland may be a heat source. In contrast, it can be concluded that the use of grassland is not a good method of climate adaption planning irrespective of the city under consideration in any climate zone.

4.2.2. Implications for urban thermal environment mitigation and cooling energy saving

As is shown in previous studies, by reducing the heat released from walls and roads [1,10] and increasing water and green vegetation [48,53] to regulate the sensible and latent heat fluxes, the UHI effect and the corresponding cooling energy consumption can be mitigated [45]. This study validates these mitigation measures by presenting SHF changes in seasonal and diurnal patterns across various landscape types. The study results showed that the SHF of the artificial impervious surfaces were significantly higher than those of the natural surfaces, which supports measures to reduce the UHI and air-conditioning energy consumption via the use of low-heat-conducting building materials and light-colored paint [10,15]. The implication of this result in the context of mitigation of urban thermal environments is that reducing the heat released by walls and roads is generally more effective than increasing the cooling of natural surfaces, although promoting urban blue and green spaces are considered a promising approach for mitigating UHI effects [54,55]. This will provide a direct basis for planners and decision-makers to mitigate the UHI effect and reduce cooling energy consumption.

As a cost-effective, environment-friendly, and politically acceptable approach [56], however, urban blue and green space still play an important role in UHI mitigation, cooling energy conservation, and sustainable urban development [17–19,57]. This study showed that water has the lowest SHF compared to trees and grassland in different seasons, which suggests that the use of water can be a better approach to the UHI mitigation compared to the green vegetation [47]. However, as discussed above, for the regulation role of the SHF, latent heat fluxes, and shading effect, the use of the urban tree is also a good method of climate adaption [42,51]. Furthermore, considering the integrated ecosystem services between water and trees in cities (climate regulation is part of ecosystem services) [47], we think that the use of urban trees is a better choice than water, especially considering the fact that bodies of water have a warming effect in summer evenings [42,58]. Furthermore, according to the SHF results of grassland in different seasons and based on the previous studies [3,9], we proposed that grassland is not a good method of climate adaption. This means that when planning an urban green space, a tree-covered green space should be given preference over a grass-covered green space. Nevertheless, we also suggest that grass-covered green roofs can be designed to change the thermal properties of walls and reduce the heat released from buildings, thus reducing the buildings' cooling energy consumption [16,53].

In addition, many previous studies on thermal environments have been focused on the comparison of surface temperatures in different regions (and urban landscapes) and obtaining surface temperature profiles [13,26,41,59]. However, in this study, the ratios of SHF were quantified for typical urban landscapes in different temporal patterns. For instance, in summer, the contribution ratio of roads, grassland, trees, walls, and water to the thermal environment is $9.7:-1:-3.4:22.1:-5.5$. The SHF ratio of grassland in different seasons (spring-autumn, summer, and winter) is $-1:-0.4:4.7$. These results could provide a reference for the improvement of urban energy balance and heat flux research [22] and numerical simulation studies of the energy conservation property of green vegetation [17,18]. It can also help to explain the mechanisms of heat flux in different urban landscapes, which RS data-based studies have not explained well.

4.3. Limitations and further study

Some limitations of this study are necessary to be mentioned. Firstly, the research design of this study has some drawbacks. For example, the experimental measurements collected from the wall did not include all the directions (only a wall facing south was considered in this study), which may result in an overestimation of the surface temperature (and SHF) of the wall; measurements should be obtained for all directions in future studies. In addition, the impact of the height of the surrounding buildings on the results was not considered in this study. Moreover, because the experimental measurements were conducted only during the daytime, further experiments could include nighttime measurements as well as more representative study sites and longer time periods. Secondly, the SHF results may be affected by other factors that require further consideration. For example, the SHF may be affected by anthropogenic heat, and this is required to be taken into consideration in future studies [6]. Besides, further study should consider the effect of forced convection to obtain a more accurate SHF result. Thirdly, this study only considers the SHF of different urban landscapes, and in the next step, latent heat fluxes are required to be included to comprehensively track the urban heat flux and surface energy balance. In future research, calculations of the SHF changes per unit area of the urban landscape can be used to estimate the global surface heat changes in a given area. By combining this information with data from the actual area, the thermal environment information for that area can be obtained. Hence, these estimated results are more accurate than the results obtained using remote sensing or weather-station data.

It should be noted that we measured the heat change on the surface of the building and obtained the vertical temperature, which cannot be

collected via remote sensing. We demonstrated the influence of the building wall on the thermal environment and accurately described the 3D structure. Based on the above results, it was found that the contribution of the landscape to the thermal environment is different, especially the thermal contribution of the wall in the vertical direction. Therefore, when modeling the urban thermal environment using the surface temperature, differences in the various landscapes and their proportions should be considered, and these ratios should be used as parameters to adjust the model to obtain accurate results [24]. In addition, the temporal dynamics of different landscape contributions should be considered when using models to simulate thermal environments.

5. Conclusions

UHI effect increases cooling energy consumption in urban areas and it is deeply affected by the heat flux dynamics of different urban landscapes. However, we still lack a clear understanding of the quantitative contribution rate and the underlying mechanism of typical urban landscapes to urban heat dynamics, especially in seasonal and diurnal patterns. This restricts us to take effective measures to alleviate the UHI effect and reduce cooling energy consumption. Therefore, with the employment of thermal infrared camera and portable meteorological instruments, the pattern (contribution) of SHF changes in typical urban landscapes in different temporal patterns in Beijing was quantitatively analyzed.

Specifically, this study revealed that: (1) the impervious surfaces of walls and roads are heat sources, trees and water are heat sinks during all seasons; while grassland served as a heat sink and source in summer, spring-autumn, and winter, respectively. Therefore, after compared with the results of many previous (RS-based) studies, we concluded that grassland is not a recommended method for climate adaption. (2) The seasonal variation of the SHF of the wall is the largest, followed by that of water, while that of trees is minimal. The highest SHF differences between the urban landscapes occurred between noon and 2:00 pm (local time), during which the SHF reached its maximum daily value. (3) The ratios of heat sources and sinks exhibited diurnal and seasonal variations, and the contribution of this pattern to the thermal environment varied in the forenoon and afternoon. We hence suggested that these ratios can be used as parameters for adjusting the model to obtain more reliable results when modeling the urban surface energy flux. (4) This study also demonstrates the accuracy of RS-data-based studies and aids in answering the related controversial questions and provides insights into the SHF mechanisms of different urban landscapes.

The results of this study are of great value for understanding the heat flux dynamics of different urban landscapes and achieving cooling energy savings.

Author contributions

Assistant Professor Dr. Zhaowu Yu deepened the research questions, analyzed the data, and mainly write the manuscript. Ms. Tingting Chen did the field measurement, analyzed the data, and partly contribute to writing the manuscript. Professor Dr. Ranhao Sun overall managed the study and did comments to improve the manuscript. Dr. Gaoyuan Yang edit and comment the manuscript. Dr. Wei Xie did field measurement and data analysis. Professor Dr. Henrik Vejre did some comments to improve the study and the manuscript.

Declaration of Competing Interest

The authors claim that there is no conflicts of interests.

Acknowledgements

This work was supported by the National Natural Science Foundation of China (grant no. 41922007); Open Foundation of the State Key Laboratory of Urban and Regional Ecology of China (grant no. SKLURE2019-2-6); Shanghai Key Lab for Urban Ecological Processes and Eco-Restoration (grant no. SHUES2019A01); WEL Visiting Fellowship Program.

Appendix A. Supplementary material

Supplementary data to this article can be found online at https://doi.org/10.1016/j.apenergy.2020.114724.

References

[1] Akbari H, Kolokotsa D. Three decades of urban heat islands and mitigation technologies research. Energy Build 2016;133:834–42.
[2] Oke TR, Mills G, Christen A, Voogt JA. Urban climates. Cambridge University Press; 2017.
[3] Yu Z, Yao Y, Yang G, Wang X, Vejre H. Strong contribution of rapid urbanization and urban agglomeration development to regional thermal environment dynamics and evolution. For Ecol Manage 2019;446:214–25.
[4] Sobstyl JM, Emig T, Qomi MJA, Ulm FJ, Pellenq RJM. Role of city texture in urban heat islands at nighttime. Phys Rev Lett 2018;120:108701.
[5] Churkina G, Kuik F, Bonn B, Lauer A, Grote Rd, Tomiak K, et al. Effect of VOC emissions from vegetation on air quality in berlin during a heatwave. Environ Sci Technol 2017.
[6] Sun R, Wang Y, Chen L. A distributed model for quantifying temporal-spatial patterns of anthropogenic heat based on energy consumption. J Cleaner Prod 2018;170:601–9.
[7] Santamouris M. On the energy impact of urban heat island and global warming on buildings. Energy Build 2014;82:100–13.
[8] Forman RT. Urban ecology: science of cities. Cambridge University Press; 2014.
[9] Yu Z, Yao Y, Yang G, Wang X, Vejre H. Spatiotemporal patterns and characteristics of remotely sensed regional heat islands during the rapid urbanization (1995–2015) of Southern China. Sci Total Environ 2019;674:242–54.
[10] Akbari H. Cooling our communities. A guidebook on tree planting and light-colored surfacing. Lawrence Berkeley National Laboratory; 2009.
[11] Luan X, Yu Z, Zhang Y, Wei S, Miao X, Huang ZY, et al. Sensing and social sensing data reveal scale-dependent and system-specific strengths of urban heat island determinants. Rem Sens 2020;12.
[12] Zhou W, Qian Y, Li X, Li W, Han L. Relationships between land cover and the surface urban heat island: seasonal variability and effects of spatial and thematic resolution of land cover data on predicting land surface temperatures. Landscape Ecol 2014;29:153–67.
[13] Ma Q, Wu J, He C. A hierarchical analysis of the relationship between urban impervious surfaces and land surface temperatures: spatial scale dependence, temporal variations, and bioclimatic modulation. Landscape Ecol 2016;31:1–15.
[14] Akbari H, Pomerantz M, Taha H. Cool surfaces and shade trees to reduce energy use and improve air quality in urban areas. Sol Energy 2001;70:295–310.
[15] Gilbert H, Mandel BH, Levinson R. Keeping California cool: recent cool community developments. Energy Build 2016;114:20–6.
[16] Santamouris M. Cooling the cities – a review of reflective and green roof mitigation technologies to fight heat island and improve comfort in urban environments. Sol Energy 2014;103:682–703.
[17] Kong F, Sun C, Liu F, Yin H, Jiang F, Pu Y, et al. Energy saving potential of fragmented green spaces due to their temperature regulating ecosystem services in the summer. Appl Energy 2016;183:1428–40.
[18] Wang Z-H, Zhao X, Yang J, Song J. Cooling and energy saving potentials of shade trees and urban lawns in a desert city. Appl Energy 2016;161:437–44.
[19] Santamouris M, Ban-Weiss G, Osmond P, Paolini R, Synnefa A, Cartalis C, et al. Progress in urban greenery mitigation science–assessment methodologies advanced technologies and impact on cities. J Civ Eng Manage 2018;24:638–71.
[20] Yan J, Zhou W, Jenerette GD. Testing an energy exchange and microclimate cooling hypothesis for the effect of vegetation configuration on urban heat. Agric For Meteorol 2019;279.
[21] Yu Z, Yang G, Zuo S, Jørgensen G, Koga M, Vejre H. Critical review on the cooling effect of urban blue-green space: a threshold-size perspective. Urban For Urban Gree 2020;49:126630https://doi.org/10.1016/j.ufug.2020.126630.
[22] Kuang W, Liu Y, Dou Y, Chi W, Chen G, Gao C, et al. What are hot and what are not in an urban landscape: quantifying and explaining the land surface temperature pattern in Beijing, China. Landscape Ecol 2015;30:357–73.
[23] Kim J, Hong T, Jeong J, Koo C, Jeong K. An optimization model for selecting the optimal green systems by considering the thermal comfort and energy consumption. Appl Energy 2016;169:682–95.
[24] Jim CY. Air-conditioning energy consumption due to green roofs with different building thermal insulation. Appl Energy 2014;128:49–59.
[25] Chudnovsky A, Ben-Dor E, Saaroni H. Diurnal thermal behavior of selected urban objects using remote sensing measurements. Energy Build 2004;36:1063–74.
[26] Hoyano A, Asano K, Kanamaru T. Analysis of the sensible heat flux from the exterior

surface of buildings using time sequential thermography. Atmos Environ 1999;33:3941–51.
[27] Miao S, Chen F. Enhanced modeling of latent heat flux from urban surfaces in the Noah/single-layer urban canopy coupled model. Sci China Earth Sci 2014;57:2408–16.
[28] Wu Z, Wang Y, Kong F, Sun R, Chen L, Zhan W. Analysis of the thermal characteristics of selected urban surfaces in a typical residential area based on infrared thermography. Acta Ecol Sinica 2016;36:5421–31.
[29] Kwok R. Ecology's remote-sensing revolution. Nature 2018;556:137–8.
[30] Gao J, Yu Z, Wang L, Vejre H. Suitability of regional development based on ecosystem service benefits and losses: a case study of the Yangtze River Delta urban agglomeration, China. Ecol Ind 2019;107:105579.
[31] Lin W, Yu T, Chang X, Wu W, Zhang Y. Calculating cooling extents of green parks using remote sensing: method and test. Landscape Urban Plann 2015;134:66–75.
[32] Yu Z, Xu S, Zhang Y, Jørgensen G, Vejre H. Strong contributions of local background climate to the cooling effect of urban green vegetation. Sci Rep 2018;8:6798.
[33] Yu ZW, Guo QH, Sun RH. Impact of urban cooling effect based on landscape scale: a review. Chin J Appl Ecol 2015;26:636–42.
[34] Peng J, Xie P, Liu Y, Ma J. Urban thermal environment dynamics and associated landscape pattern factors: a case study in the Beijing metropolitan region. Remote Sens Environ 2016;173:145–55.
[35] Sham JFC, Memon SA, Tommy Lo Y. Application of continuous surface temperature monitoring technique for investigation of nocturnal sensible heat release characteristics by building fabrics in Hong Kong. Energy Build 2013;58:1–10.
[36] Sham JF, Memon SA, Lo Y. Application of continuous surface temperature monitoring technique for investigation of nocturnal sensible heat release characteristics by building fabrics in Hong Kong. Energy Build 2013;58:1–10.
[37] Qin Y, Hiller JE. Understanding pavement-surface energy balance and its implications on cool pavement development. Energy Build 2014;85:389–99.
[38] Landsberg HE. The urban climate. Academic press; 1981.
[39] Ali-Toudert F, Mayer H. Numerical study on the effects of aspect ratio and orientation of an urban street canyon on outdoor thermal comfort in hot and dry climate. Build Environ 2006;41:94–108.
[40] Weng Q, Liu H, Lu D. Assessing the effects of land use and land cover patterns on thermal conditions using landscape metrics in city of Indianapolis, United States. Urban Ecosyst 2007;10:203–19.
[41] Estoque RC, Murayama Y, Myint SW. Effects of landscape composition and pattern on land surface temperature: an urban heat island study in the megacities of Southeast Asia. Sci Total Environ 2017;577:349–59.
[42] Fan H, Yu Z, Yang G, Liu TY, Liu TY, Hung CH, et al. How to cool hot-humid (Asian) cities with urban trees? An optimal landscape size perspective. Agric For Meteorol 2019;265:338–48.
[43] Song X-P, Hansen MC, Stehman SV, Potapov PV, Tyukavina A, Vermote EF, et al. Global land change from 1982 to 2016. Nature 2018;1.
[44] Yu Z, Guo X, Jørgensen G, Vejre H. How can urban green spaces be planned for climate adaptation in subtropical cities? Ecol Ind 2017;82:152–62.
[45] Yu Z, Fryd O, Sun R, Jorgensen G, Yang G, Özdil N, et al. Where and how to cool? An idealized urban thermal security pattern model. Landscape Ecol 2020. https://doi.org/10.1007/s10980-020-00982-1.
[46] Yu Z, Guo X, Zeng Y, Koga M, Vejre H. Variations in land surface temperature and cooling efficiency of green space in rapid urbanization: the case of Fuzhou city, China. Urban Urban Greening 2018;29:113–21.
[47] Yang G, Yu Z, Jørgensen G, Vejre H. How can urban blue-green space be planned for climate adaption in high-latitude cities? A seasonal perspective. Sustain Cities Soc 2020;53:101932https://doi.org/10.1016/j.scs.2019.101932.
[48] Gunawardena K, Wells M, Kershaw T. Utilising green and bluespace to mitigate urban heat island intensity. Sci Total Environ 2017;584:1040–55.
[49] Qiu GY, Zou Z, Li X, Li H, Guo Q, Yan C, et al. Experimental studies on the effects of green space and evapotranspiration on urban heat island in a subtropical megacity in China. Habitat Int 2017;68:30–42.
[50] O'Malley C, Piroozfar P, Farr ER, Pomponi F. Urban Heat Island (UHI) mitigating strategies: a case-based comparative analysis. Sustain Cities Soc 2015;19:222–35.
[51] Jiao M, Zhou W, Zheng Z, Wang J, Qian Y. Patch size of trees affects its cooling effectiveness: a perspective from shading and transpiration processes. Agric For Meteorol 2017;247:293–9.
[52] Oliveira S, Andrade H, Vaz T. The cooling effect of green spaces as a contribution to the mitigation of urban heat: a case study in Lisbon. Build Environ 2011;46:2186–94.
[53] Solcerova A, van de Ven F, Wang M, Rijsdijk M, van de Giesen N. Do green roofs cool the air? Build Environ 2017;111:249–55.
[54] Gaffin SR, Rosenzweig C, Kong AY. Adapting to climate change through urban green infrastructure. Nat Clim Change 2012;2:704.
[55] Ellison D, Morris CE, Locatelli B, Sheil D, Cohen J, Murdiyarso D, et al. Trees, forests and water: cool insights for a hot world. Global Environ Change 2017;43:51–61.
[56] Martins TA, Adolphe L, Bonhomme M, Bonneaud F, Faraut S, Ginestet S, et al. Impact of urban cool Island measures on outdoor climate and pedestrian comfort: simulations for a new district of Toulouse, France. Sustain Cities Soc 2016;26:9–26.
[57] Yu Z. The cooling effect of urban green infrastructure: from how to where. Copenhagen: University of Copenhagen; 2018.
[58] Akbari H, Bell R, Brazel T, Cole D, Estes M, Heisler G, et al. Reducing urban heat Islands: compendium of strategies urban heat Island basics. US Environmental Protection Agency; 2008. p. 1–22.
[59] Bernales A, Antolihao J, Samonte C, Campomanes F, Rojas R, Silapan J. Modelling the relationship between land surface temperature and landscape patterns of land use land cover classification using multi linear regression models. ISPRS-Int Arch Photogram, Rem Sens Spatial Inform Sci 2016;41:851–6.